AGU PUBLICATIONS

JGR

Journal of Geophysical Research: Solid Earth

RESEARCH ARTICLE
10.1002/2012JB009826

Key Points:
- M > 8.6 subduction thrust earthquakes triggering M > 5.5 crustal events likely
- M > 5.5 crustal quakes triggered atop M > 7.5 subduction thrust ruptures likely

Correspondence to:
J. Gomberg,
gomberg@usgs.gov

Citation:
Gomberg, J., and B. Sherrod (2014), Crustal earthquake triggering by modern great earthquakes on subduction zone thrusts, *J. Geophys. Res. Solid Earth*, *119*, 1235–1250, doi:10.1002/2012JB009826.

Received 9 OCT 2012
Accepted 24 JAN 2014
Accepted article online 6 FEB 2014
Published online 24 FEB 2014

Crustal earthquake triggering by modern great earthquakes on subduction zone thrusts

Joan Gomberg[1] and Brian Sherrod[1]

[1]U.S. Geological Survey, Department of Earth and Space Sciences, University of Washington, Seattle, Washington, USA

Abstract Among the many questions raised by the recent abundance of great ($M > 8.0$) subduction thrust earthquakes is their potential to trigger damaging earthquakes on crustal faults within the overriding plate and beneath many of the world's densely populated urban centers. We take advantage of the coincident abundance of great earthquakes globally and instrumental observations since 1960 to assess this triggering potential by analyzing centroids and focal mechanisms from the centroid moment tensor catalog for events starting in 1976 and published reports about the *M*9.5 1960 Chile and *M*9.2 1964 Alaska earthquake sequences. We find clear increases in the rates of crustal earthquakes in the overriding plate within days following all subduction thrust earthquakes of $M > 8.6$, within about ±10° of the triggering event centroid latitude and longitude. This result is consistent with dynamic triggering of more distant increases of shallow seismicity rates at distances beyond ±10°, suggesting that dynamic triggering may be important within the near field too. Crustal earthquake rate increases may also follow smaller $M > 7.5$ subduction thrust events, but because activity typically occurs offshore in the immediately vicinity of the triggering rupture plane, it cannot be unambiguously attributed to sources within the overriding plate. These observations are easily explained in the context of existing earthquake scaling laws.

1. Introduction

The largest earthquakes of the last half century—*M*9.2 1964 Alaska, *M*9.1 2004 Aceh-Andaman, *M*9.5 1960 and *M*8.8 2010 Chile, and M9.0 (Tohoku-oki) Japan—each occurred as thrust events on subduction zone plate interfaces and triggered potentially damaging earthquakes ($M > \sim 5.5$) within the overriding plate. If located near population centers, these smaller but closer triggered earthquakes may be more hazardous than even the largest subduction thrust event. While raising the public's concerns about the potential for triggered crustal earthquakes, the apparent burst in $M > 8.3$ subduction thrust earthquakes [*Michael*, 2011; *Parsons and Geist*, 2012] also has provided an unprecedented wealth of observations for assessing empirically this triggering potential. The global centroid moment tensor (CMT) [*Global Central Moment Tensor(CMT) Catalog*, 2011] provides a key set of observations, which form the basis for this study. We were particularly motivated to address these concerns for the Cascadia subduction zone, where earthquake hazards threaten significant U.S. populations and where others have inferred from geological observations that a past *M*~9 subduction thrust earthquake may have triggered a cluster of $M > \sim 6.5$ crustal earthquakes between A.D. 800–1100. We illustrate the similarity between the geologic settings of Cascadia and Japan in Figure 1 and describe how we addressed this concern in Cascadia in a companion paper [*Sherrod and Gomberg*, 2014]. Although the results of this study of the modern record suggest that previous inferences of possible triggering of the A.D. 800–1100 cluster of $M > \sim 6.5$ crustal earthquakes by a great Cascadia megathrust earthquake were plausible, *Sherrod and Gomberg* [2014] concluded that this cluster most probably was not triggered, although they also could not rule out the possibility of smaller, triggered crustal earthquakes.

Previous studies have also studied major earthquake triggering potential empirically, examining seismicity rate changes globally, but none have focused specifically on the potential for plate interface, subduction thrust events to trigger earthquakes in the overriding plate. Moreover, some previous studies offer somewhat contradictory results. For example, *Parsons and Velasco* [2011] examined seismicity rates for $5 < M < 7$ events of all types following $M > 7$ earthquakes globally at distances ranging from the near to far fields (i.e., within a few to well beyond distances comparable to a few multiples of the triggering earthquake's rupture dimension, respectively). They found rate increases only within the first 20–30 h and 300–1000 km of the triggering event but not beyond, i.e., within the near field only. The *Parsons and Velasco* [2011] results contrast with those of the study of *Pollitz et al.* [2012], who also looked at $M > 5.5$ earthquakes, but beyond 1500 km from the posited

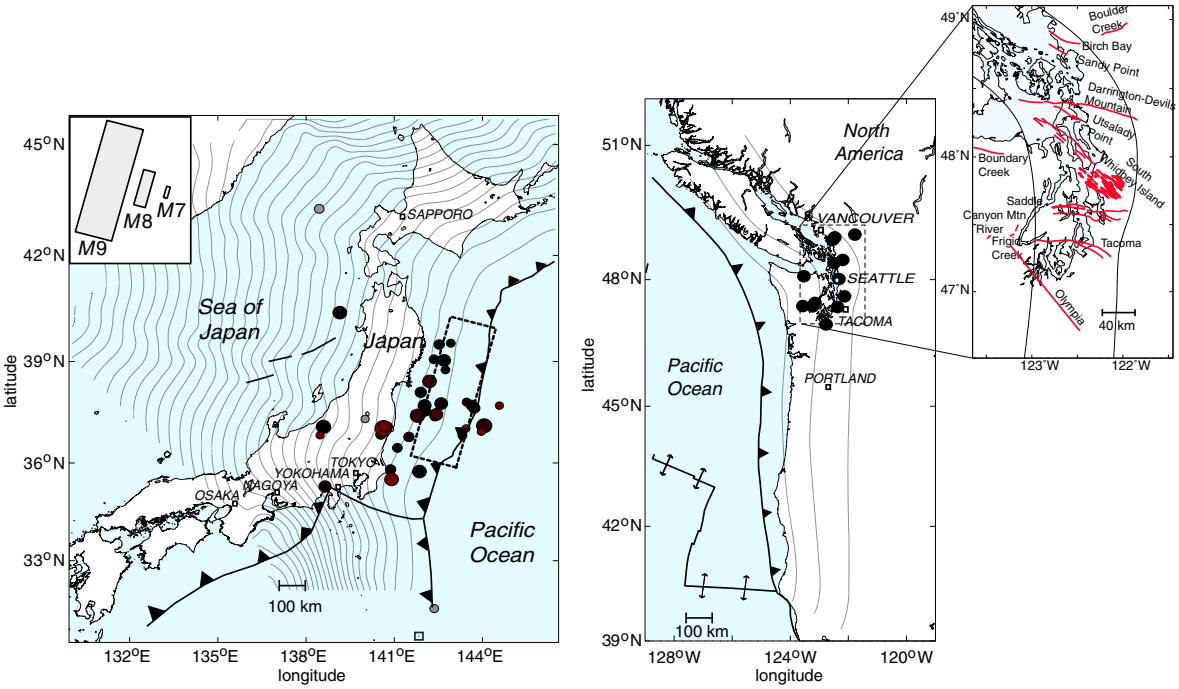

Figure 1. Comparison of settings of crustal triggering in Japan with that of posited triggering in Cascadia. (left) Tectonic map of Japan and centroid latitudes and longitudes of $M > 5.5$ earthquakes within 1 year before and in the 6 weeks after the *M*9.0 2011 Tohoku-oki, Japan earthquake. Solid circles are crustal earthquake centroid latitudes and longitudes (gray before Tohoku-oki, shading from black to brown in the first 2 months), with symbol sizes scaled to magnitudes. The dashed rectangle roughly outlines the surface projection of the Tohoku-oki rupture plane. The inset shows visually how the *M*9 Tohoku-oki rupture area (largest gray rectangle, plotted at the same scale as in the map) might scale if it was a *M*8 or *M*7 earthquake assuming a logarithmic scaling with magnitude (explained in the text). (right) Tectonic map of Cascadia with approximate epicenters of $M > \sim 6.5$ crustal earthquakes in the Puget Sound region within the last 16,000 years (solid circles) [*Sherrod and Gomberg*, 2014]. The rupture area of the last *M*9.0 earthquake in 1700 probably spanned the entire length of the contours and at least to the 20 km depth contour. In both maps, contours of the depth to the plate interface at 20 km increments, with trench axes shown as the line with triangles.

triggering event, in the far field. *Pollitz et al*. [2012] found that all (six) $M > 8.5$ earthquakes were followed by statistically significant rate increases, at distances where *Parsons and Velasco* [2011] concluded they did not exist. All but the 2012 *M*8.6 east Indian Ocean earthquake in the *Pollitz et al*.'s [2012] study were subduction thrust events. In both of these studies, rate increases occurred within the first 2 days of the triggering earthquake. We examine triggering within the *Parsons and Velasco*'s [2011] definition of the near-field distances only and restrict triggered events to $M > 5.5$ earthquakes on crustal faults.

A primarily empirical approach to assessing triggering potential has several important advantages over modeling studies. In only a few instances, there are sufficient constraints for conclusive model-based studies, particularly within the hanging wall above thrust faults (especially when blind), where the stress change patterns are complex, and aftershocks are distributed diffusely with varied mechanisms [*Stein et al*., 1994]. The *M*9.0 2011 Tohoku-oki earthquake sequence illustrates some of the challenges, noting that it is among the most well-constrained sequences because of an extraordinary abundance of high-quality data and attention. *Nettles et al*.'s [2011] study of the Tohoku-oki sequence emphasized the wide variety of focal mechanisms among the "nonconforming" aftershocks (i.e., those within the overriding plate). *Toda et al*. [2011a, 2011b] modeled static Coulomb stress changes to assess their potential to trigger Tohoku-oki crustal aftershock activity. The results of the study of *Toda et al*. [2011b] indicate that the Tohoku-oki main shock relaxed the stresses in the majority of the areas exhibiting rate changes (53%), but still the rates of small, mostly shallow earthquakes increased in twice the number of areas that experienced decreases. *Toda et al*. [2011a] examined Coulomb stress triggering of the seven largest ($M > 5.4$), most exotic (off the plate interface), and remote aftershocks, using the CMT catalog and found that 57% were brought closer to failure on both nodal planes. While they interpret the 86% that were brought closer to failure on at least one nodal plane as indication of success, an alternative view is that 86% exhibited inconsistent stress changes on at least one nodal plane. While we do not question the inferences of *Toda et al*. [2011a, 2011b], we suggest that the choice of results emphasized also complicates the inferences drawn. Moreover, the nonuniqueness likely will

be greater for studies of other sequences elsewhere, which lack the detailed observations available for the Tohoku-oki sequence.

Finally, some studies combine empirical (statistical) approaches with physical models, such as those invoking "epidemic-type aftershock sequence" and related models [see *Helmstetter et al*., 2005, and references therein] that assume aftershock sequences arise from a cascade of triggered earthquakes with spatial and temporal patterns that follow particular parametric relations. A related approach avoids assumption of the latter, but all the approaches in this class assume that the parameters describing the earthquakes are drawn from a single distribution [*Marsan and Nalbant*, 2005; *Marsan and Lengliné*, 2008], which is demonstrably not true when considering both earthquakes on subduction zone plate interface and within the overriding plate. Multiple distributions may be considered, but typically, the problem of estimating the needed parameters is too underdetermined for solution. Thus, we exploit the abundance of great earthquakes since 1960 to assess this triggering potential globally using a purely empirical approach.

2. The Modern Earthquake Record of Crustal Triggering by Subduction Thrust Earthquakes

2.1. Method

Our test for a probable causal connection between a posited triggering $M > 7.5$ earthquake and a significantly increased rate of $M > 5.5$ crustal earthquakes in the overriding plate is premised on the fact that each are low-probability occurrences, and thus, the joint probability of them both happening within a month of one another by chance is extremely low. Our test criteria are very conservative, noting that a month is a tiny fraction of the recurrence intervals of tens to thousands of years for $M > 5.5$ earthquakes. Undoubtedly, triggering occurs over longer times and distances than those considered, but consideration of longer spatial or temporal windows increases theprobability of occurrence of both the triggering and triggered events and thus makes inferences of causal connections more difficult to establish. In this section, we describe how we verified significant crustal seismicity rate changes by comparing the cumulative rates of both numbers of earthquakes and of moment release to background rates (rate increases identified in terms of numbers of events almost always correspond to significant increases in moment release rate as well).

We assess the potential for great subduction thrust earthquakes to trigger crustal earthquakes in the overriding plate using the modern seismological record characterized in the CMT catalog, which includes a total of 13 $M > 8.0$ and 2 $M > 9.0$ subduction thrust earthquakes from the start of the catalog in 1976 until 11 April 2011. For each of the subduction thrust earthquakes, we assess triggering of $M > 5.5$ crustal earthquakes in the overriding plate because shallow earthquakes of this size are potentially damaging and because the post-1976 catalogs of them are likely complete [*Felzer et al*., 2004]. We examine the $M > 5.5$ crustal earthquakes within $\pm 10°$ of the centroid latitude and longitude of the posited triggering great interplate earthquake. A single spatial window was chosen rather than scaling by the rupture dimension of the triggering event to avoid biases (i.e., tailoring the data set based on a prior scaling assumptions) and to be large enough to include distances that exceeded several rupture lengths of the largest triggering earthquake considered. Ten degrees is approximately the same as the limit beyond which the triggered seismicity was no longer observed by *Parsons and Velasco* [2011] and that they suggest to separate the near and far fields of the largest triggering events and is the shortest distance considered by *Pollitz et al*. [2012] in their study of "remotely" triggered seismicity (see Discussion section below).

We identified crustal earthquakes as those shallower than 50 km and above the plate interface by >20 km with any mechanism or if within 20 km of the interface with mechanisms that differ from pure thrusts (rake differences exceeding 30). The latter assumes that earthquakes on the interface will slip in accordance with stresses related to plate convergence. The depths of the plate interfaces are taken from *Hayes et al*. [2012] (see also http://earthquake.usgs.gov/research/data/slab/#models, last accessed December 2011). These interface models do not come with quantitative estimates of their uncertainties, but we suggest that conservatively, on average, the uncertainties may be of the same order as the contour interval of 20 km. Near the trench, these criteria do not discriminate crustal earthquakes within the subducting and overriding plates, and because of the uncertainties in the depths of the earthquake and the plate interface, acknowledge that some events may be misclassified.

Table 1. $M > 8.0$ Interplate Earthquake Locations, Origin Times and Mechanisms

	Hypocenter				Origin Time		Nodal Plane 1			Nodal Plane 2		
Country	Latitude	Longitude	Depth (km)	Magnitude	Date	Time	Stk	Dip	Rk	Stk	Dip	Rk
Chile	−38.16	72.20	25	9.5	22/5/60	19:11:14						
Alaska	61.04	−147.73	25	9.2	28/3/64	3:36						
Ecuador (Temuco)	2.32	−78.81	20	8.1	12/12/79	08:00:07	30	16	118	181	76	83
Mexico (Michoacan)	17.91	−101.99	21	8.0	19/9/85	13:18:24	301	18	105	106	73	85
Chile	−24.17	−70.74	29	8.0	30/7/95	05:11:56	354	22	87	177	68	91
Mexico (Jalisco)	19.34	−104.8	15	8.0	9/10/95	15:36:28	302	9	92	120	81	90
Indonesia (Biak)	−0.67	136.62	15	8.2	17/2/96	06:00:02	103	11	69	305	80	94
Peru	−17.28	−72.71	30	8.4	23/6/01	20:34:23	310	18	63	159	74	98
Japan (Tokachi-oki)	42.21	143.84	28	8.3	25/9/03	19:50:38	250	11	132	28	82	83
Aceh-Andaman	3.09	94.26	29	9.1	26/12/04	01:01:09	329	8	110	129	83	87
Sumatra (Nias)	1.67	97.07	26	8.6	28/3/05	16:10:31	333	8	118	125	83	86
Kuril Islands	46.71	154.33	14	8.3	15/11/06	11:15:08	215	15	92	33	75	89
Solomon Islands	−7.79	156.34	14	8.1	1/4/07	20:40:38	333	37	121	117	59	69
Peru (Ica)	−13.73	−77.04	34	8.0	15/8/07	23:41:57	321	28	63	171	65	104
Sumatra (southern Sumatra)	−3.78	100.99	24	8.5	12/9/07	11:11:15	328	9	114	123	82	86
Chile	−35.98	−73.15	23	8.8	27/2/10	06:35:14	19	18	116	172	74	82
Japan (Tohoku-oki)	37.52	143.05	20	9.1	11/3/11	05:47:32	203	10	88	25	80	90

We also examined the scaling of triggering potential with earthquake size by analyzing the crustal earthquake activity following the $M > 7.5$ subduction thrust earthquakes within the catalog windowed for each great earthquake. Finally, we considered earthquake sequences surrounding the two largest, but pre-CMT earthquakes in recorded history, the 1960 *M*9.5 Chile and 1964 *M*9.2 Alaska earthquakes because they are constrained by locally recorded instrumental data, albeit sparse. Table 1 contains the characteristics of these 17 $M > 8.0$ earthquakes.

Our approach shares many aspects with the global studies of *Parsons and Velasco* [2011] and *Pollitz et al*. [2012], as already noted in the Introduction and described below. For each of the aforementioned 1976 and later subduction thrust earthquakes, we infer triggering when one of the two criteria are satisfied. In the first, the monthly rate increases immediately (within a month) following the triggering event's origin time. To infer triggering, we require that the observed monthly rate of the $M > 5.5$ crustal earthquakes estimated just after the posited triggering event exceeds twice the standard deviation of the mean monthly rate; we show plots of these quantities for the years surrounding each posited triggering earthquake (see sections below). As in the works of *Parsons and Velasco* [2011] and *Pollitz et al*. [2012], we estimate the mean rate and its variability using a Monte Carlo approach, randomly sampling monthly intervals from the entire catalog to estimate the distribution of rates (characterized by their means and standard deviations). These reference estimates are conservative, as they preserve some of the inherent clustering in the catalog and thus maximize the variability. The second triggering criterion requires the posited triggering event to be followed within a month by an exceptionally "large" crustal earthquake, with a magnitude within the top 5% of the range for the entire catalog for the region considered. Thus, triggering may involve just one or a few crustal earthquakes.

2.2. Results

2.2.1. The 2011 *M*9.0 Tohoku-oki and Other Earthquakes in Japan

The triggering of widespread earthquakes in the overriding plate by the *M*9.0 Tohoku-oki earthquake was extraordinary, because of its clarity and proximity to dense populations [*Asano et al*., 2011; *Ishibe et al*., 2011; *Kato et al*., 2011; *Toda et al*., 2011a, 2011b; *Yoshida et al*., 2012]. Note that the significant crustal rate increase that commenced within a day of the Tohoku-oki earthquake was composed of numerous events in the overriding plate, several of which had $M > 6$ and were near population centers (Figures 1a and 2). The 1983 *M*8.3 Tokachi-oki earthquake lacked any crustal earthquakes for the following months (Figure 1b). Only one of the six $7.5 < M < 8.0$ interface earthquakes within ±10° of either the Tokachi-oki and Tohoku-oki earthquakes may have triggered crustal earthquakes in the overlying plate; the *M*7.7 on 28 December 1994 was followed by the *M*6.9 Kobe crustal earthquake, but a 19 day delay and epicentral separation of ~5° make a causal connection highly speculative (Figure 2a). Although before the dawn of modern seismic monitoring and our study period, *Kakehi and Iwata* [1992] and *Kikuchi et al*. [2003] suggest that the *M*8.1 Tonankai interface earthquake promoted the occurrence of the 1945

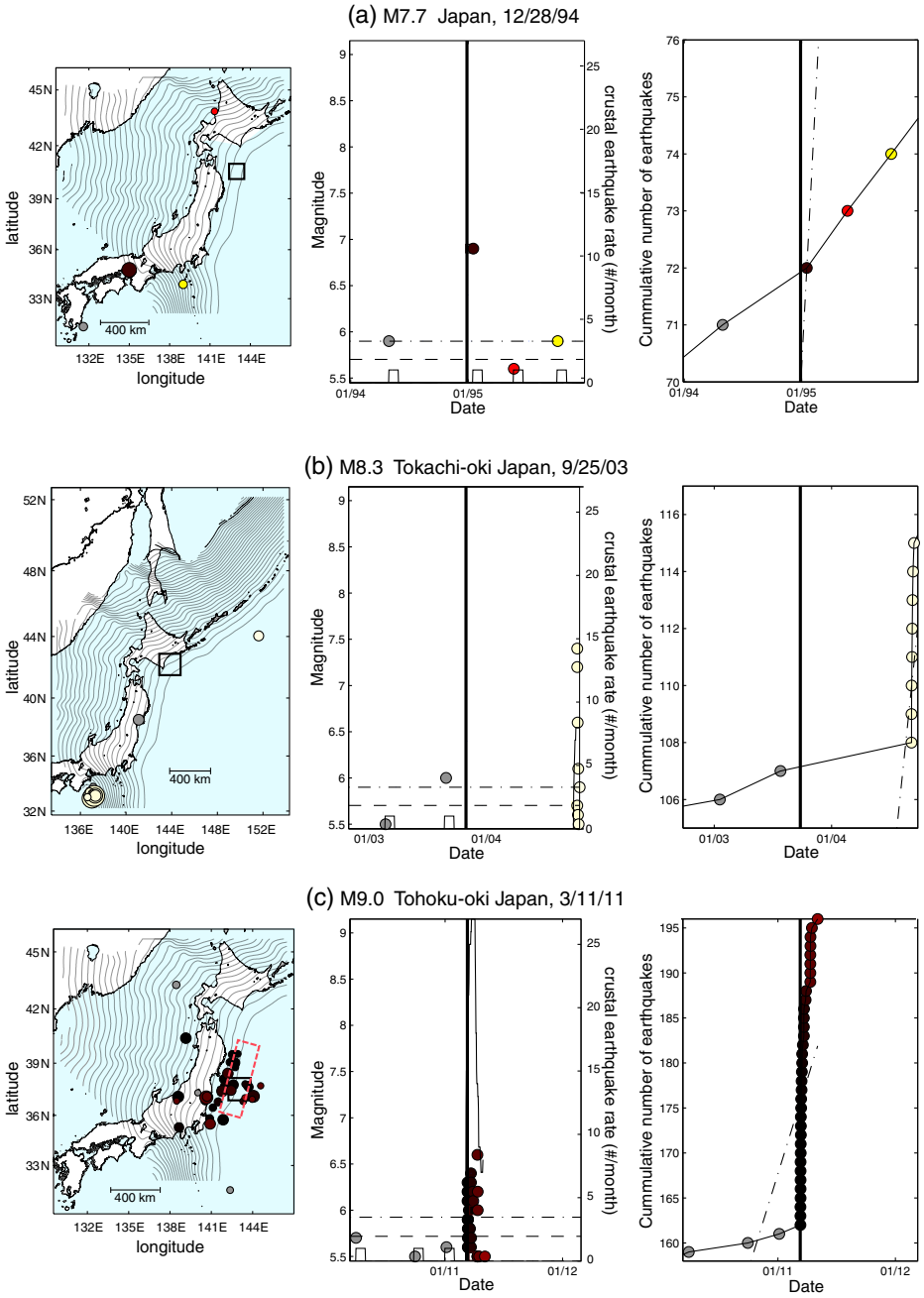

Figure 2. Examples of spatial and temporal crustal earthquake rate changes for earthquakes in Japan. (a–c) Rates are shown surrounding three posited triggering earthquakes in Japan. The magnitude and date of the posited triggering events are labeled. (left) Maps of centroid latitudes and longitudes of $M > 5.5$ earthquakes surrounding posited triggering earthquakes within ±10° and 1 year before and after. Earthquakes within the crust before the triggering event shown as gray circles and after as circles colored according to the time. The color coding is the same as in the time histories to the right, and symbol sizes scale with earthquake magnitude. Contours show depth to the plate interface at 20 km intervals. For each posited triggering earthquake, maps show the surface projection of the centroid (open square) and only for $M > 8.6$ events the approximate rupture plane (red dashed polygons). (middle) Magnitudes (left axis) versus time (x axis) of the same earthquakes plotted in the map with the same symbol type and color scheme as the map to the left. The monthly rate of crustal earthquakes calculated in a moving window is plotted as the black outlined bar graph. Dashed horizontal lines indicate one and two standard deviations from the mean rate calculated for the entire catalog, from 1 January 1976 to 11 April 2011, estimated by sampling monthly intervals randomly (i.e., ~95% of all monthly rates are within the two standard deviation bounds). (right) Cumulative seismic number of earthquakes, respectively, for 1 year before and after the posited triggering earthquake (center vertical line). Dashed lines show the mean plus two standard deviations of the earthquake rates estimated from monthly sampling. Cumulative moment plots are not shown and have the same behavior as the cumulative numbers.

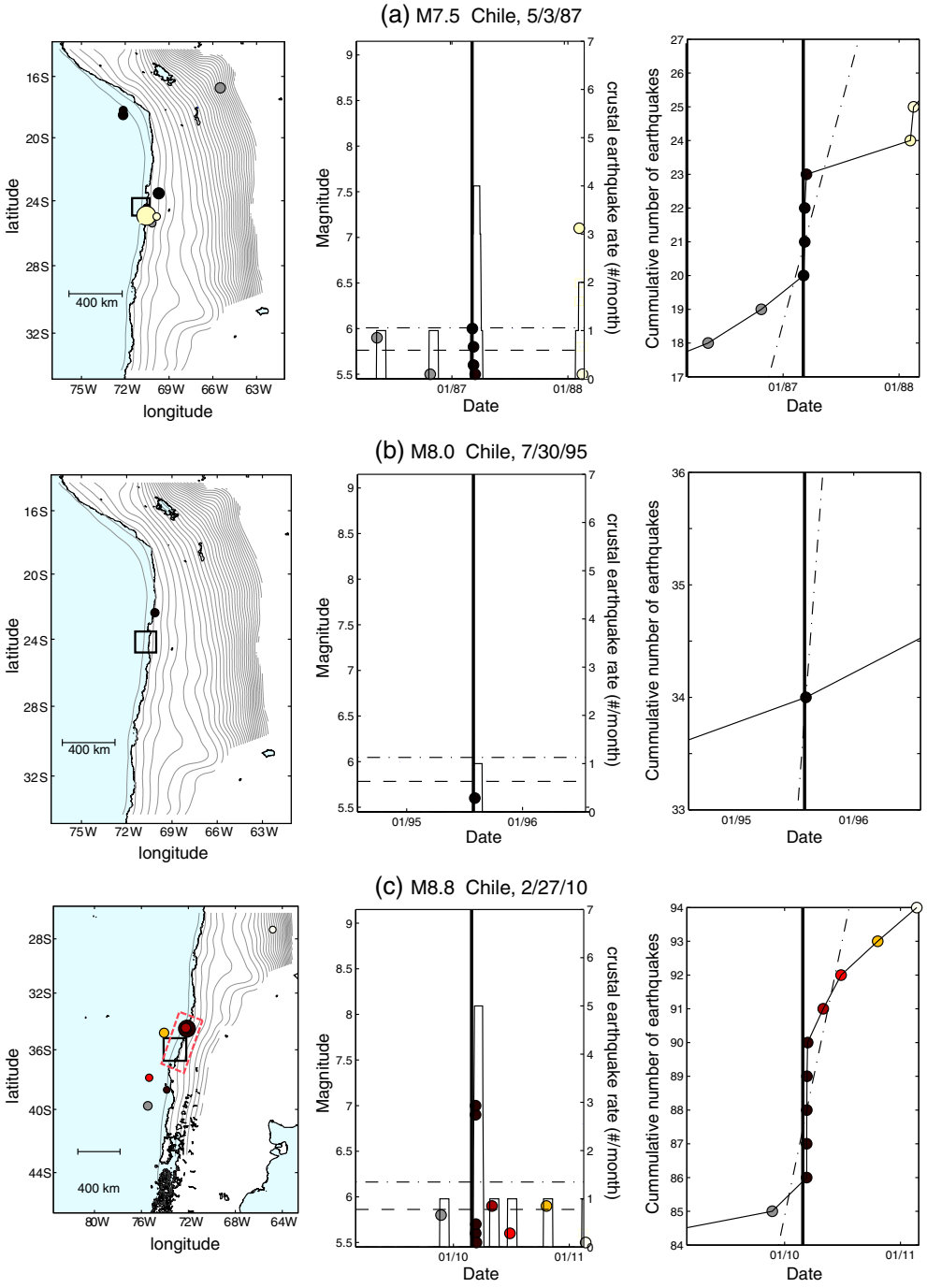

Figure 3. Crustal earthquake rates surrounding the origin times of $M > 7.5$ interface earthquakes in Chile. Same format as Figure 2 but for posited triggering earthquakes in Chile.

*M*7.1 Mikawa crustal earthquake in the overriding plate 37 days later, given the recurrence interval of host crustal fault of 20,000 to 30,000 years [*Okada*, 2006]. However, the rupture planes of these two earthquakes were likely separated by only tens of kilometers, making a causal connection more likely than for the aforementioned 1994 pair.

2.2.2. The 1960 *M*9.5, 2010 *M*8.8, and Other Earthquakes in Chile

The 1995 *M*8.0 interface earthquake did not trigger a rate change or an extraordinarily large crustal earthquake (Figure 3), but within the same region, the *M*7.5 interface event on 5 March 1987 triggered a

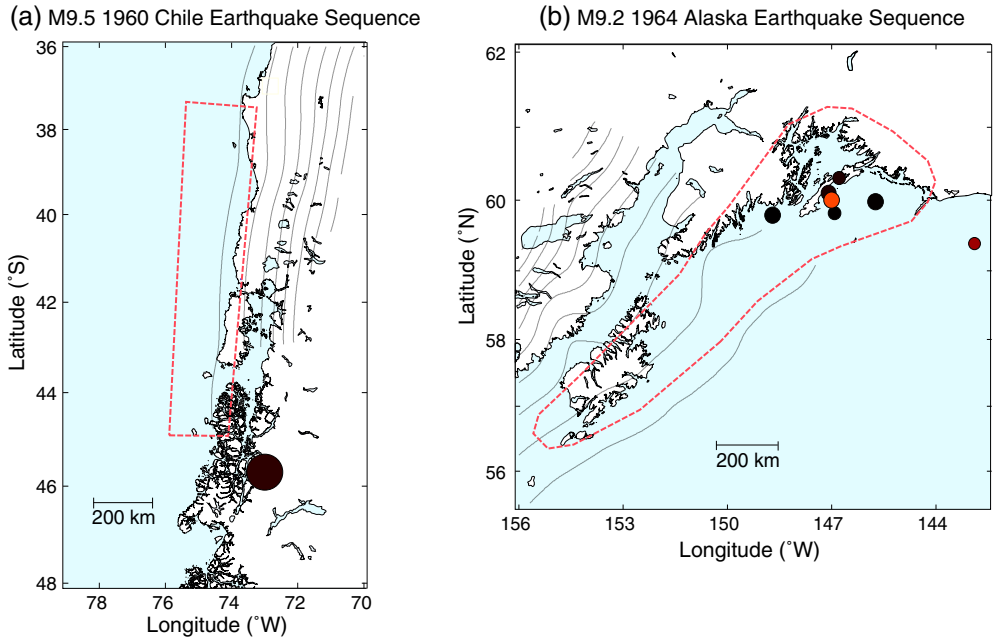

Figure 4. Centroid latitudes and longitudes of earthquakes within 1 year after the 1960 *M*9.5 Chile and 1964 *M*9.2 Alaska earthquakes plotted in the same format as the maps in Figure 2. (a) Crustal seismicity surrounding of the 1960 *M*9.5 Chile earthquake was studied by *Cifuentes* [1989]. (b) Aftershocks of the 1964 *M*9.2 Alaska earthquake was studied by *Doser et al.* [1999, 2002] in two regions above the rupture zone, centered on Kodiak Island and Prince William Sound and extending several hundreds of kilometers into the interior Alaska.

crustal rate increase and included a *M*6.0 earthquake clearly located in the overriding plate. The 2010 *M*8.8 subduction thrust event triggered both a crustal rate increase and large events just above the interface rupture but still within the overriding plate; a pair of *M*6.9 and *M*7.0 normal-faulting crustal earthquakes occurred on previously assumed inactive faults and caused significant damage in the nearest city of Pichilemu [*Ryder et al.*, 2012; *Rietbrock et al.*, 2012]. *Rietbrock et al.* [2012] also noted increased seismicity rates in the outer-rise region. The 1960 *M*9.5 earthquake sequence was documented by *Cifuentes* [1989], who reported that the first crustal event was a M_s7.0 earthquake located offshore at the trench that could have been in the subducting plate, but she also reported two other crustal aftershocks (all others were likely at or below the plate interface), the first being a M_s~7.5 event 14.6 days after the *M*9.5 earthquake (Figure 4a) and the second with m_b~5.4 and 5.5 years later. In contrast to the 2010 crustal triggering near Pichilemu on an assumed inactive fault [*Ryder et al.*, 2012], *Cifuentes* [1989] suggests that these crustal aftershocks plausibly ruptured the Liquine-Ofqui fault system, which is a major active strike-slip system straddling the volcanic arc and accommodating oblique plate convergence [*Moreno et al.*, 2008].

2.2.3. The 2004 Aceh-Andaman Islands and Other Regional Earthquakes

Only the 2004 *M*9.1 and 2005 *M*8.6 interplate earthquakes triggered clear widespread crustal rate increases and large crustal events (Figure 5), at distances of hundreds of kilometers from each rupture plane. These crustal rate increases occurred mostly to the north and south of the 2004 and 2005 ruptures, respectively. While these two triggering earthquakes are separated by only 4 months, two spatially and temporally separated crustal rate increases can be distinguished (Figures 5a and 5b), suggesting that the second surge was triggered by the second thrust event. Curiously, the 2007 *M*8.5 earthquake well to the south of the 2004 and 2005 great events did not trigger any seismicity increases in the overriding plate, but within the ±10° surrounding region, a crustal rate increase did follow a *M*7.7 interface event on 17 July 2006 (Figure 5d). However, all events were just above the triggering rupture plane and could have been within the subducting plate.

2.2.4. The 1964 *M*9.2 and Other Earthquakes in Alaska

Information about the earthquakes that followed the *M*9.2 earthquake on 28 March 1964 are published in the studies of *Doser et al.* [1999, 2002]. *Doser et al.* [1999, 2002] examined two regions above the *M*9.2 earthquake

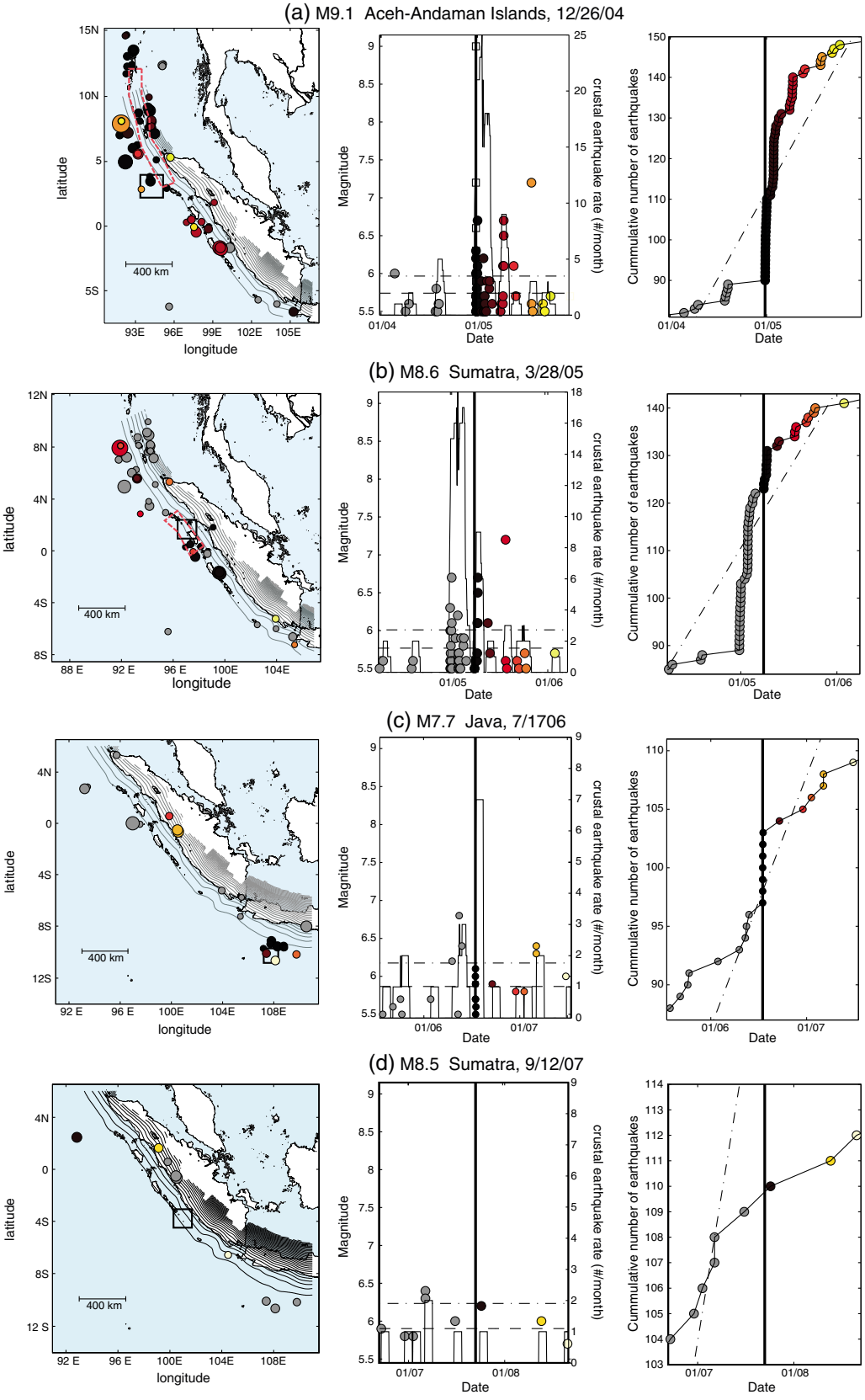

Figure 5. Crustal earthquake rates surrounding the origin times of $M > 7.5$ interface earthquakes in Sumatra, Java, and the Aceh-Andaman Islands. Same format as Figure 2.

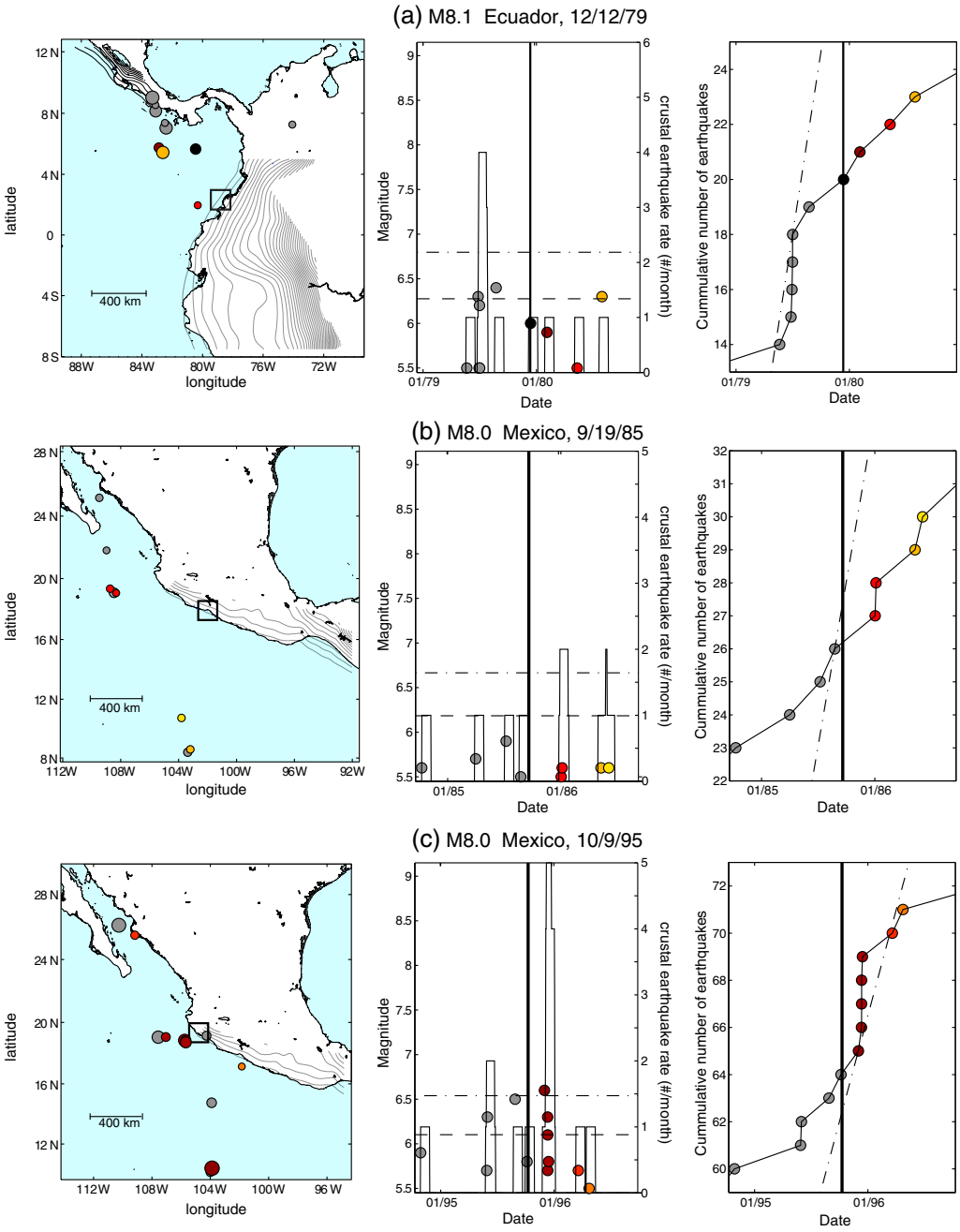

Figure 6. Crustal earthquake rates surrounding the origin times of $M > 7.5$ interface earthquakes in regions where triggering did not occur or is questionable at best. Same format as Figure 2.

rupture zone, centered on Kodiak Island and Prince William Sound and extending several hundreds of kilometers into interior Alaska (Figure 4b). The completeness of their catalogs is difficult to assess and so we considered all the events they cataloged (the smallest event has *M*5.3). *Doser et al.* [1999, 2002] noted several crustal earthquakes, but the first near Kodiak Island did not occur until 1967. However, in the Prince William Sound region, the largest crustal events occurred within the first day following the *M*9.2 earthquake (the first was *M*6.1); all others were within the first 90 days, and all were directly above the *M*9.2 event's rupture plane. The only $M > 7.5$ earthquakes since 28 March 1964 were crustal events themselves (from the CMT catalog), one in 1988 outboard of the trench offshore within the subducting plate and the other in 2002 in interior Alaska.

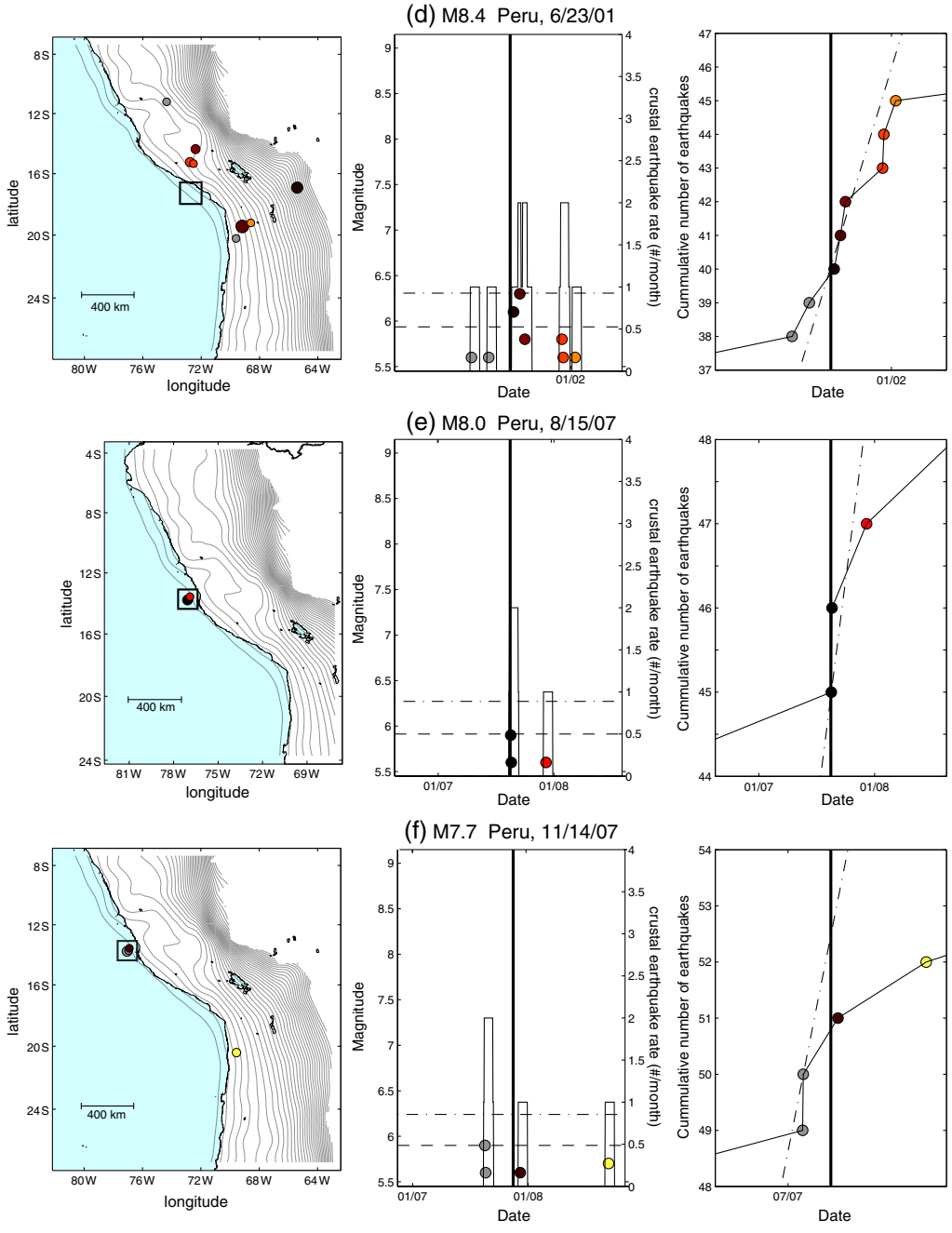

Figure 6. (continued)

2.2.5. Earthquakes in Costa Rica, Ecuador, Mexico, Peru, Indonesia, the Solomon Islands, and the Kuril Islands

No triggering followed the great 1979 *M*8.1 Ecuador, 1985 *M*8.0 and 1995 *M*8.0 Mexico, and 2001 *M*8.4 Peru interface earthquakes (Figures 6a–6d). The rates of crustal earthquakes increased nearly immediate (within 1 day) for numerous other interface earthquakes, but just above the interface ruptures so that the crustal events could be in the subducting plate. For the $7.5 < M < 8.0$ interface ruptures, this occurred for the 1992 *M*7.6 Costa Rica and 1989 *M*7.5 and 2002 *M*7.6 Indonesia earthquakes (Figures 6g–6j). The same is true for the 2007 *M*8.0 Peru (Figure 6e), 1996 *M*8.2 Indonesia (Figure 6i), 2007 *M*8.1 Solomon Islands, and 2006 *M*8.3 Kuril Islands interface earthquakes (Figures 6k–6m). Although clearly not in the overriding plate, notably the *M*8.3 Kuril Islands event triggered a *M*8.0 crustal earthquake on the outer rise of the

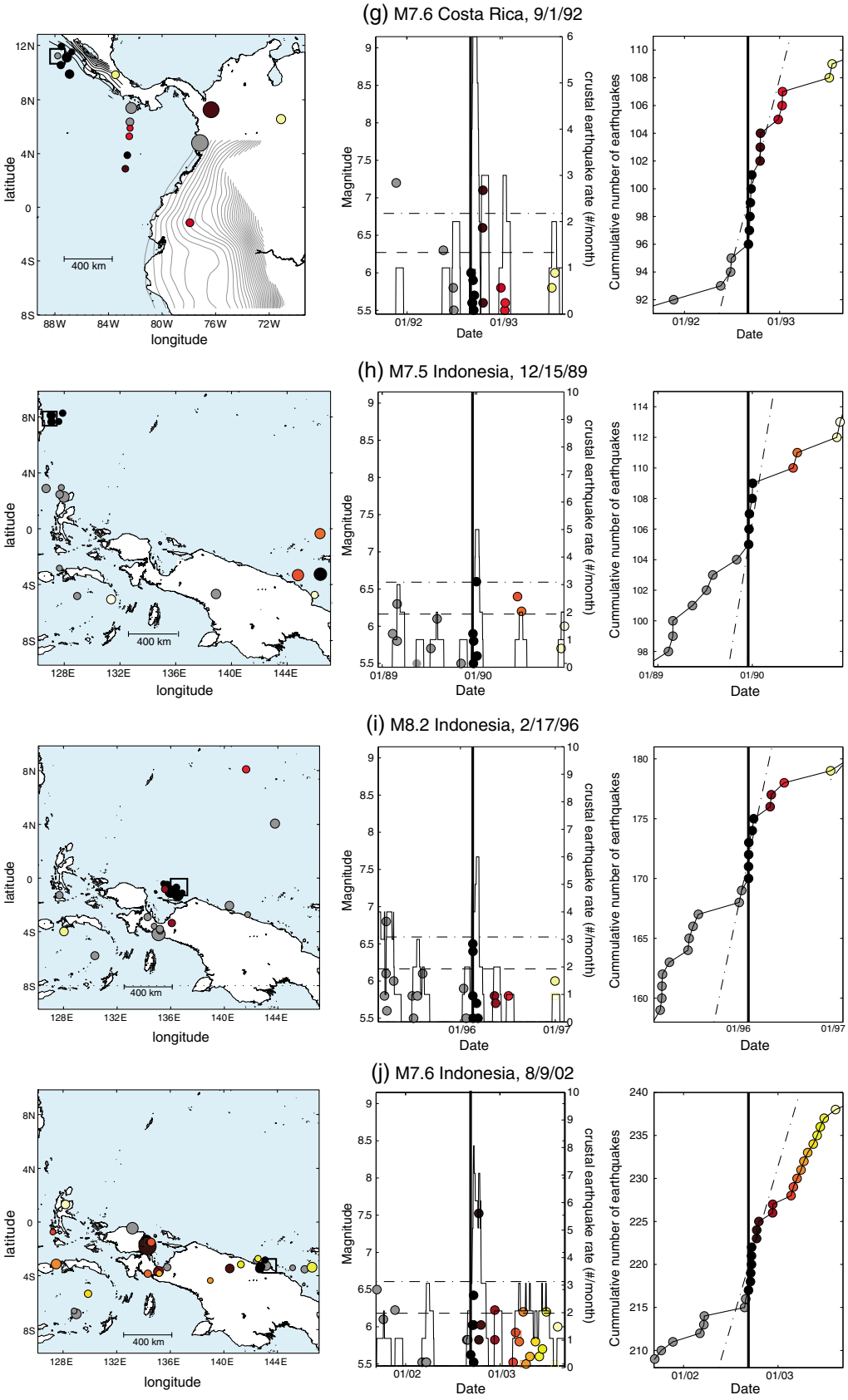

Figure 6. (continued)

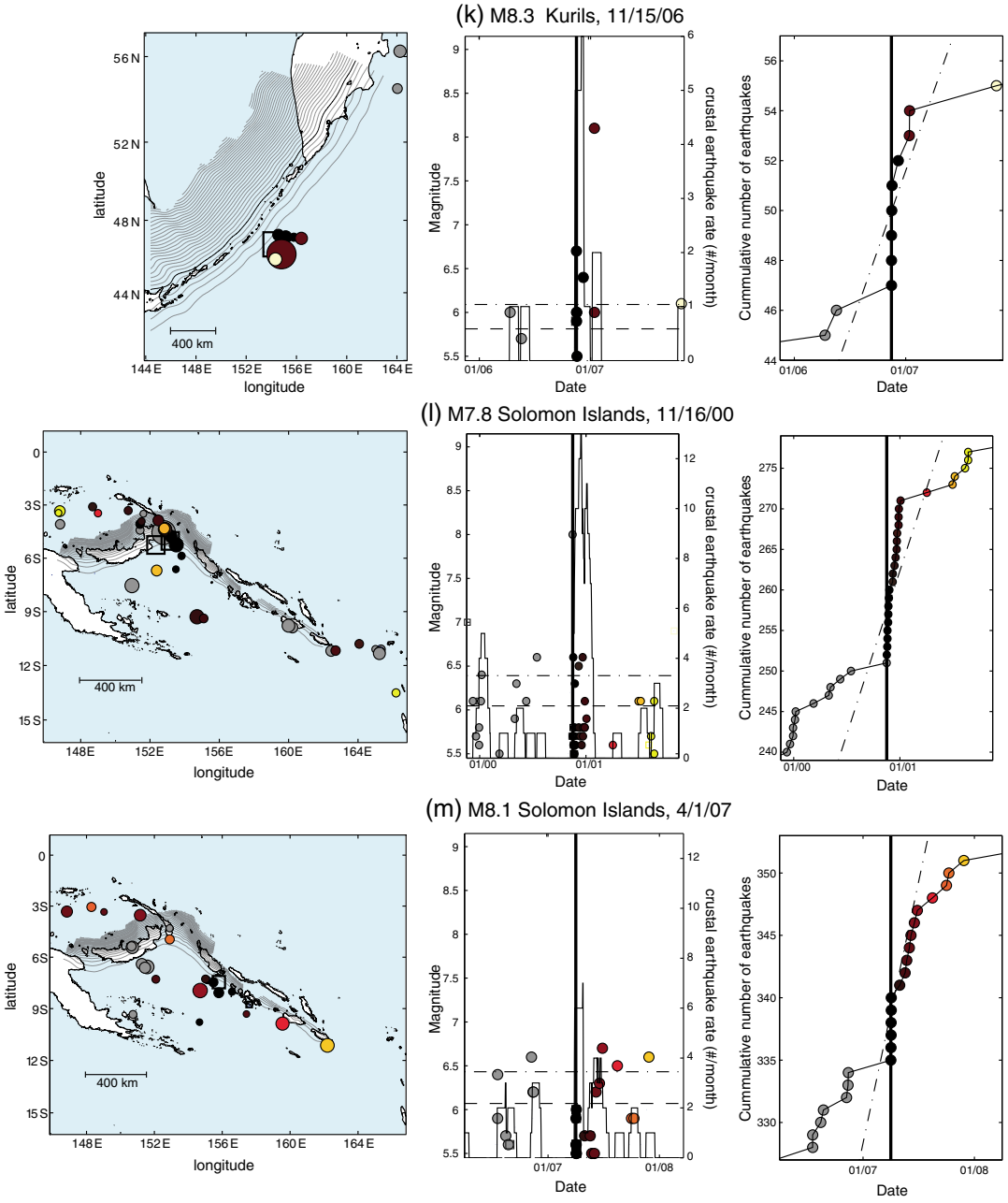

Figure 6. (continued)

subducting plate. The triggering of the two crustal earthquakes in the overriding plate by the 2001 *M*8.4 Peru interface events is questionable given the delay to the first one by just over a month (Figure 6d). The most curious case perhaps is the *M*7.8 Solomon Islands interface earthquake of 16 November 2000 that was preceded 3 h earlier by a *M*8.0 crustal event within just a few degrees in the overriding plate and then followed by another *M*7.8 interface earthquake 38 h later (Figure 6l). A clear crustal rate increase followed both.

3. Discussion and Conclusions

All six $M > 8.6$ interplate earthquakes since 1960 triggered $M > 5.5$ crustal earthquakes within days and distances comparable to a few multiples of the dimensions of the triggering events and in most cases on faults not previously identified as significant seismogenic structures (Figure 7). We also find that globally, smaller interface earthquakes ($M > \sim 7.5$) also trigger crustal earthquakes but mostly in offshore areas and

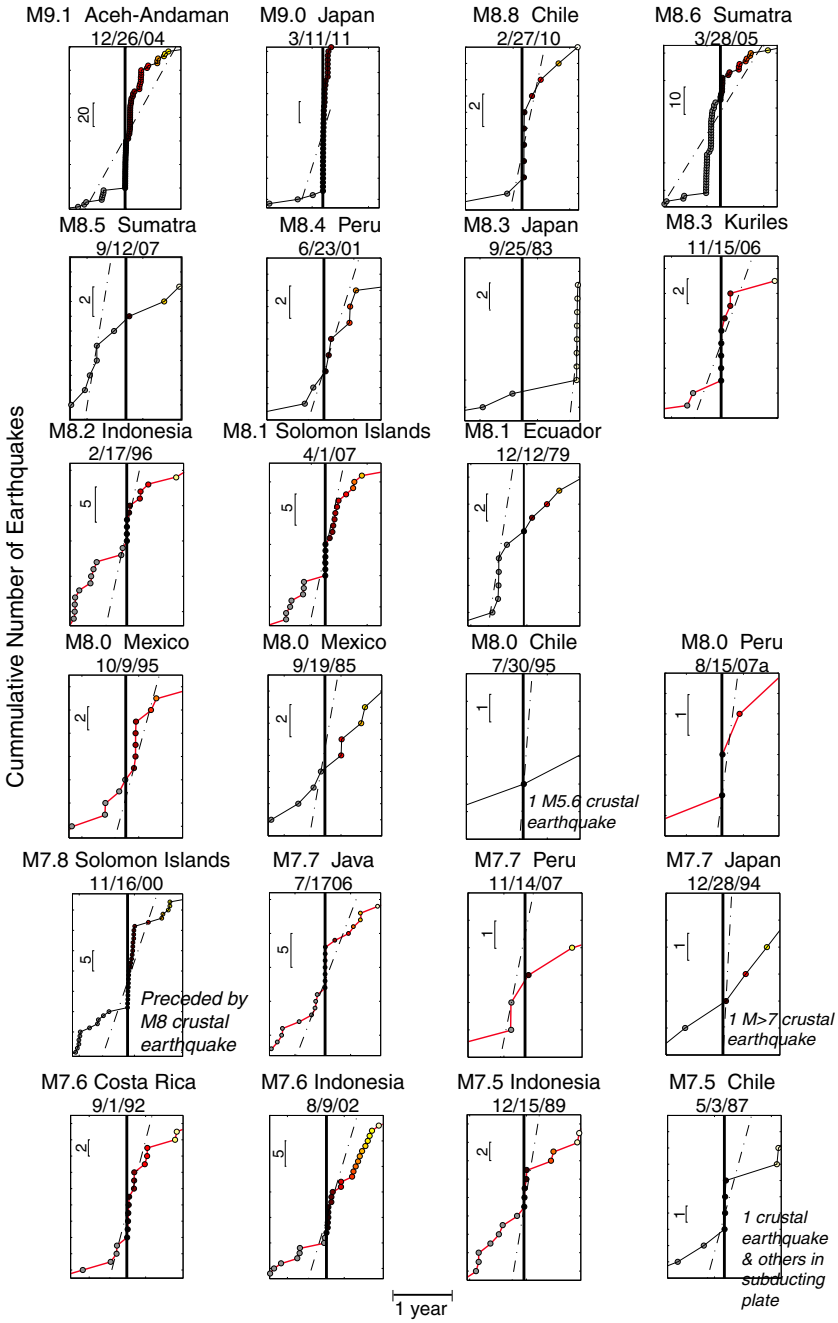

Figure 7. Crustal earthquake rates surrounding the origin times of $M > 7.5$ interface earthquakes. The cumulative numbers (scale bars on each plot) of $M > 5.5$ crustal earthquakes in the CMT catalog within ±10° and 1 year before and after all $M > 7.5$ interface earthquakes studied (vertical lines at their origin times, same format as the right frames of Figure 2). The only earthquakes for which the crustal rate at the time of the posited triggering event unambiguously increases to more than two standard deviations from the long-term average rates (dashed) are those with $M > 8.6$. Cases in which the crustal seismicity after the posited triggering interface earthquakes cannot be distinguished from activity within the subducting plate because the events locate just above the interface earthquakes, or on or beyond the outer rise, are shown in red. Ambiguous triggering or other noteworthy cases are annotated and discussed in the text.

often on the outer rise (noted in Figure 7 in red), and while the shaking from these poses little hazard, they can generate tsunamis [*Lay et al.*, 2011].

The patterns of triggered activity we observe do not imply any change in the scaling of source processes of earthquakes with size, but instead, most of the crustal earthquakes may be considered to be aftershocks of

the subduction thrust events. Aftershocks often are defined as earthquakes within the region that very approximately correspond to distances from the triggering earthquake comparable to its rupture dimension. This physically based definition is consistent with empirically defined aftershock zones within which the seismicity rate surrounding a main shock is elevated above a background rate [*Marsan and Lengliné*, 2008]. A distance range comparable to a rupture dimension also defines the "near field," where the main shock-generated deformation field includes both significant permanent or "static" and radiated wave or "dynamic" components. Beyond the near-field dynamic, stress changes attenuate more slowly than static changes, but even at some far-field distances, both have been shown to explain triggering observations [*Cotton and Coutant*, 1997; *Gomberg et al*., 2003; *Ziv*, 2006; *Gomberg and Felzer*, 2008; *van der Elst and Brodsky*, 2010; *Marsan and Lengliné*, 2010].

Physically, triggering requires the intersection of a collection of near-failure faults and a region of stress changes sufficient to promote failure on such primed faults. The stress changes within the near field of a fault that has just slipped are close to the maximum limited by the strength of the fault [*Brune*, 1970, 1976] and thus may be approximated as uniform and nearly maximal (and thus sufficient to trigger). The near-field region scales with the rupture area [*Cotton and Coutant*, 1997; *Gomberg and Felzer*, 2008], which scales logarithmically with magnitude (Figure 1 inset) [*Kanamori and Anderson*, 1975; *Felzer et al*., 2004; *Helmstetter et al*., 2005, 2006; *Marsan and Lengliné*, 2008; *Blaser et al*., 2010; *Strasser et al*., 2010]. In other words, the areas encompassed by near-field deformations, which appear able to trigger an earthquake on a fault ripe for failure, grow logarithmically with magnitude (Figure 1 inset). Thus, the largest earthquake's deformation field encompasses a huge region and most probably, one or several crustal faults ripe for being triggered. Figures 1–5 show the approximate rupture areas of the $M > 8.6$ earthquakes studied and that most of the crustal earthquakes within the overriding plate that followed within days occurred within distances roughly comparable to the rupture dimensions. The rupture dimensions of $M > 8.6$ earthquakes are hundreds of kilometers or more so that their near-field regions, where triggering is highly probable, cover much of the areas considered (±10° of the triggering centroids). Although some triggering appears to occur beyond near-field distances (e.g., following the Tohoku-oki earthquake, Figures 1 and 2), as we noted above, we cannot attribute this definitively to a particular type of stress or physical change because these changes vary gradually (i.e., sharp boundaries do not separate the near and far fields) and because triggering should be viewed probabilistically.

We have chosen to examine $M > 5.5$ crustal earthquakes because of the need for catalog completeness and because we are most interested in potentially damaging events. However, triggering of a rate increase of $M < 5.5$ crustal earthquakes may imply an increased probability of $M > 5.5$ events too, given that the numbers of earthquakes typically scale systematically with magnitude (e.g., follow a Gutenberg-Richter distribution in which the number of earthquakes decreases logarithmically with increasing magnitude). In other words, we acknowledge that a lower magnitude cutoff and observation of increased rates of $M < 5.5$ earthquakes might reveal the increased probabilities of $M > 5.5$ events, even when the associated increased rate of $M > 5.5$ earthquakes may not be sufficient to be observed within the time interval examined. This extrapolation is not guaranteed however because the scaling may apply only to $M < 5.5$ events (i.e., faults large enough to host $M > 5.5$ earthquakes may not exist, or the transition to "characteristic" scaling [*Schwartz and Coppersmith*, 1984] may occur at or below *M*5.5). A detailed study of local catalogs, beyond the scope of this study, would be required to determine if the triggered rate changes of smaller earthquakes implied heightened probabilities of $M > 5.5$ earthquakes in the regions studied. Results of several previous studies that have used local network data to examine rate changes following subduction thrust earthquakes highlight the challenges in extrapolating from increases in the rates of small-magnitude crustal earthquakes, $M <$ ~5, to estimate the likelihood of larger ones, at least within the first few months following the triggering event. *Toda et al*. [2011b] reported widespread rate changes of $M_j > 0$ (Japanese Meteorological Agency magnitude scale), of mostly shallow earthquakes within the first 3 months after the *M*9.0 Tohoku-oki earthquake, out to ~300 km from the inland edge of the rupture surface. They showed that of the 14 geographic boxes where rates increased, half contained $M > 5$ earthquakes and half did not. *Rietbrock et al*. [2012] reported that most crustal seismicity in the immediate aftermath of the *M*8.8 2010 Chile earthquake concentrated in the area of the *M*6.9 and *M*7.0 Pichilemu crustal aftershocks, but they also noted increases of only small-magnitude (local magnitudes <3) seismicity rates beneath the active volcanic front.

Interestingly, several cases suggest that a crustal earthquake may trigger an interface event, the first of which met our data selection criteria and includes a *M*7.8 interface earthquake in the Solomon Islands in 2000

preceded by a *M*8.0 crustal earthquake by only 3 h and well within distances of the rupture dimensions of both (Figure 6l). A more remarkable case is a *M*8.0 outer-rise earthquake followed within minutes by a pair of *M*7.8 interplate events in the Tonga subduction zone [*Lay et al*., 2010] (none captured by our selection method), although the very slow, largely aseismic beginnings of the latter may imply that they were actually the triggering events [*Beavan et al*., 2010]. While not a source of hazardous ground motions to populations onshore and of concern in this study, the prevalence of crustal events triggered immediately above the interface rupture and at or seaward of the trench axis on the outer rise should be noted because these may generate tsunamis, as evidenced by the *M*8.0 outer-rise earthquake that followed the 2006 *M*8.3 Kuril Islands interface earthquake (Figure 6k) [*Lay et al*., 2009].

Finally, our results agree with those of *Parsons and Velasco* [2011] related to triggering of $M > 5$ earthquakes in the near field (distances <1500 km), although they did not distinguish among event types. Consistent with their results, ours indicate that triggering of crustal $M > 5.5$ earthquakes may be nearly guaranteed for all $M > 8.6$ subduction thrust earthquakes at near-field distances. However, the *Parsons and Velasco* [2011] results from the far field contrast with those of *Pollitz et al*. [2012], as only the latter find that $M > 8.5$ events triggered $M > 5.5$ earthquakes. *Pollitz et al*. [2012] suggest that this contrast may just indicate that far-field triggering is rare, although this seems hard to reconcile with their observing it in all cases examined. If we consider the *Pollitz et al*. [2012] observations and inferences of far-field dynamic triggering, we infer that the fact that we see triggering for the same class of events, but in the near field, may imply that dynamic triggering is important at all distances.

Acknowledgments
We are grateful to Rob Witter, Art Frankel, two anonymous reviewers, and the Associate Editor for their thoughtful reviews. The authors also thank Brian Atwater, who contributed numerous ideas and suggestions and participated in thought-provoking discussions about the topics covered in this paper.

References

Asano, Y., T. Saito, Y. Ito, K. Shiomi, H. Horose, T. Matsumoto, S. Aoi, S. Hori, and S. Sekiguchi (2011), Spatial distribution and focal mechanisms of aftershocks of the 2011 off the Pacific coast of Tohoku earthquake, *Earth Planets Space*, *63*, 669–673.

Beavan, J., X. Wang, C. Holden, K. Wilson, W. Power, G. Prasetya, M. Bevis, and R. Kautoke (2010), Near-simultaneous great earthquakes at Tongan megathrust and outer rise in September 2009, *Nature*, *466*, 959–964, doi:10.1038/nature09292.

Blaser, L., F. Kruger, M. Ohrnberger, and F. Scherbaum (2010), Scaling Relations of Earthquake Source Parameter Estimates with Special Focus on Subduction Environment, *Bull. Seismol. Soc. Am.*, *100*, 2914–2926, doi:10.1785/0120100111.

Brune, J. N. (1970), Tectonic stress and the spectra of seismic shear waves from earthquakes, *J. Geophys. Res.*, *75*, 4997–5009.

Brune, J. N. (1976), The physics of earthquake strong motion, in *Seismic Risk and Engineering Decisions*, edited by C. Lomnitz and E. Rosenblueth, pp. 141–177, Elsevier, New York.

Cifuentes, I. L. (1989), The 1960 Chilean earthquakes, *J. Geophys. Res.*, *94*, 665–680.

Cotton, F., and O. Coutant (1997), Dynamic stress variations due to shear faults in plane-layered medium, *Geophys. J. Int.*, *128*, 676–688, doi:10.1111/j.1365-246X.1997.tb05328.x.

Doser, D. I., A. M. Veilleux, and M. Velasquez (1999), Seismicity of the Prince William Sound Region for over thirty years following the 1964 great Alaskan earthquake, *Pure Appl. Geophys.*, *154*, 593–632.

Doser, D. I., W. A. Brown, and M. Velasquez (2002), Seismicity of the Kodiak Island region (1964-2002) and its relation to the 1964 great Alaskan earthquake, *Bull. Seismol. Soc. Am.*, *92*, 3269–3292.

Felzer, K. R., R. E. Abercrombie, and G. Ekstrom (2004), A common origin for aftershocks, foreshocks, and multiplets, *Bull. Seismol. Soc. Am.*, *94*, 88–98, doi:10.1785/0120030069.

Global CMT Catalog (2011), [Available at www.globalcmt.org/CMTsearch.html], last accessed May, 2011.

Gomberg, J., and K. Felzer (2008), A model of earthquake triggering probabilities and application to dynamic deformations constrained by ground motion observations, *J. Geophys. Res.*, *113*, B10317, doi:10.1029/2007JB005184.

Gomberg, J., P. Bodin, and P. A. Reasenberg (2003), Observing earthquakes triggered in the near field by dynamic deformations, *Bull. Seismol. Soc. Am.*, *93*(1), 118–138.

Hayes, G. P., D. J. Wald, and R. L. Johnson (2012), Slab1.0: A three−dimensional model of global subduction zone geometries, *J. Geophys. Res.*, *117*, B01302, doi:10.1029/2011JB008524.

Helmstetter, A., Y. Y. Kagan, and D. D. Jackson (2005), Importance of small earthquakes for stress transfers and earthquake triggering, *J. Geophys. Res.*, *110*, B05S08, doi:10.1029/2004JB003286.

Helmstetter, A., Y. Y. Kagan, and D. D. Jackson (2006), Comparison of short-term and time-independent earthquake forecast models for southern California, *Bull. Seismol. Soc. Am.*, *96*, 90–106, doi:10.1785/0120050067.s.

Ishibe, T. K., K. S. Shimazaki, and H. Tsuruoka (2011), Change in seismicity beneath the Tokyo metropolitan area due to the 2011 Pacific coast of Tohoku earthquake, *Earth Planets Space*, *63*, 731–735.

Kakehi, Y., and T. Iwata (1992), Rupture process of the 1945 Mikawa earthquake as determined from strong motion records, *J. Phys. Earth*, *40*, 635–655.

Kanamori, H., and D. Anderson (1975), Theoretical basis of some empirical relations in seismology, *Bull. Seismol. Soc. Am.*, *65*, 1073–1095.

Kato, A., S. Sakai, and K. Obara (2011), A normal-faulting seismic sequence triggered by the 2011 off the Pacific coast of Tohoku earthquake: Wholesale stress regime changes in the upper plate, *Earth Planets Space*, *63*, 5–748.

Kikuchi, M., M. Nakamura, and K. Yoshikawa (2003), Source rupture processes of the 1944 Tonankai earthquake and the 1945 Mikawa earthquake from low-gain seismograms, *Earth Planets Space*, *55*, 159–172.

Lay, T., H. Kanamori, C. J. Ammon, A. R. Hutko, K. Furlong, and L. Rivera (2009), The 2006-2007 Kuril Islands great earthquake sequence, *J. Geophys. Res.*, *114*, B11308, doi:10.1029/2008JB006280.

Lay, T., C. J. Ammon, H. Kanamori, L. Rivera, K. D. Koper, and A. R. Hutko (2010), The 2009 Samoa-Tonga great earthquake triggered doublet, *Nature*, *466*, 964–968, doi:10.1038/nature09214.

Lay, T., C. Ammon, H. Kanamori, M. Kim, and L. Xue (2011), Outer trench-slope faulting and the 2011 Mw 9.0 off the Pacific coast of Tohoku earthquake, *Earth Planets Space*, *63*(7), 713–718, doi:10.5047/eps.2011.05.006.

Marsan, D., and O. Lengliné (2008), Extending earthquakes' reach through cascading, *Science*, *319*(5866), 1076–1079.

Marsan, D., and O. Lengliné (2010), A new estimation of the decay of aftershock density with distance to the mainshock, *J. Geophys. Res.*, *115*, B09302, doi:10.1029/2009JB007119.

Marsan, D., and S. S. Nalbant (2005), Methods for measuring seismicity rate changes: A review and a study of how the Mw7.3 Landers Earthquake affected the aftershock sequence of the Mw6.1 Joshua Tree earthquake, *Pure Appl. Geophys.*, *162*, 1151–1185, doi:10.1007/s00024-004-2665-4.

Michael, A. J. (2011), Random variability explains apparent global clustering of large earthquakes, *Geophys. Res. Lett.*, *38*, L21301, doi:10.1029/2011GL049443.

Moreno, M. S., J. Klotz, D. Melnick, H. Echtler, and K. Bataille (2008), Active faulting and heterogeneous deformation across a megathrust segment boundary from GPS data, south central Chile (36–39_S), *Geochem. Geophys. Geosyst.*, *9*, Q12024, doi:10.1029/2008GC002198.

Nettles, M., G. Ekstrom, and H. Koss (2011), Moment-tensor analysis of the 2011 of the Pacific Coast of Tohoku Earthquake and its larger foreshocks and aftershocks, *Earth Planets Space*, *63*, 519–523.

Okada, A. (2006), Tectonic features and characteristics of the faults associated with the 1945 Mikawa earthquake, *Active Fault Res.*, *26*, 163–192.

Parsons, T., and A. A. Velasco (2011), Absence of remotely triggered large earthquakes beyond the mainshock region, *Nature Geosci.*, *4*, 312–316, doi:10.1038/ngeo1110.

Parsons, T., and E. L. Geist (2012), Were global M > 8.3 earthquake time intervals random between 1900 and 2011?, *Bull. Seismo. Soc. Am.*, *102*, 1583–1592, doi:10.1785/0120110282.

Pollitz, F., R. S. Stein, V. Sevilgen, and R. Burgmann (2012), The 11 April 2012 east Indian Ocean earthquake triggered large aftershocks worldwide, *Nature*, *490*, 250–253, doi:10.1038/nature111504.

Rietbrock, A., I. Ryder, G. Hayes, C. Haberland, D. Comte, S. Roecker, and H. Lyon-Caen (2012), Aftershock seismicity of the 2010 Maule Mw = 8.8, Chile, earthquake: Correlation between co-seismic slip models and aftershock distribution?, *Geophys. Res. Lett.*, *39*, L08310, doi:10.1029/2012GL051308.

Ryder, I., R. Rietbrock, K. Kelson, R. Burgmann, M. Floyd, A. Socquet, C. Vigny, and D. Carrizo (2012), Large extensional aftershocks in the continental forearc triggered by the 2010 Maule earthquake, Chile, *Geophys. J. Int.*, *188*(3), 879–890, doi:10.1111/j.1365-246X.2011.05321.x.

Schwartz, D. P., and K. J. Coppersmith (1984), Fault behavior and characteristic earthquakes: Examples from the Wasatch and San Andreas Fault zones, *J. Geophys. Res.*, *89*, 5681–5698.

Sherrod, B., and J. Gomberg (2014), Crustal earthquake triggering by pre-historic great earthquakes on subduction zone thrusts, *J. Geophys. Res. Solid Earth*, *119*, doi:10.1002/2013JB010635.

Stein, R. S., G. C. P. King, and J. Lin (1994), Stress triggering of the 1994 M = 6.7 Northridge. California, earthquake by its predecessors, *Science*, *265*, 1432–1435.

Strasser, F. O., M. C. Arango, and J. J. Bommer (2010), Scaling of the Source Dimensions of Interface and Intraslab Subduction-zone Earthquakes with Moment Magnitude, *Seismo. Res. Letts.*, *81*, 941–950, doi:10.1785/gssrl.81.6.941.

Toda, S., J. Lin, and R. S. Stein (2011a), Using the 2011 *M*w 9.0 off the Pacific coast of Tohoku Earthquake to test the Coulomb stress triggering hypothesis and to calculate faults brought closer to failure, *Earth Planets Space*, *63*, 725–730.

Toda, S., R. S. Stein, and J. Lin (2011b), Widespread seismicity excitation throughout central Japan following the 2011 M = 9.0 Tohoku earthquake and its interpretation by Coulomb stress transfer, *Geophys. Res. Lett.*, *38*, L00G03, doi:10.1029/2011GL047834.

van der Elst, N. J., and E. E. Brodsky (2010), Connecting near-field and far-field earthquake triggering to dynamic strain, *J. Geophys. Res.*, *115*, B07311, doi:10.1029/2009JB006681.

Yoshida, K., A. Hasegawa, T. Okada, T. Iinuma, Y. Ito, and Y. Asano (2012), Stress before and after the 2011 great Tohoku-oki earthquake and induced earthquakes in inland areas of eastern Japan, *Geophys. Res. Letts.*, *39*, L03302, doi:10.1029/2011GL049729.

Ziv, A. (2006), On the role of multiple interactions in remote aftershock triggering: The Landers and the Hector Mine case studies, *Bull. Seismol. Soc. Am.*, *96*, 80–89.